Development of human mesenchymal stem cells on DC sputtered titanium nitride thin films

M. MANSO-SILVAN*, J. M. MARTÍNEZ-DUART
Departamento de Física Aplicada, Universidad Autónoma de Madrid, 28049 Madrid, Spain

S. OGUETA, P. GARCÍA-RUIZ
Departamento de Biología Molecular, Universidad Autónoma de Madrid, 28049 Madrid, Spain

J. PÉREZ-RIGUEIRO
Departamento de Ciencia de Materiales, ETSI Caminos Canales y Puertos, Universidad Politécnica de Madrid, 28040 Madrid. Spain
E-mail: miguel.manso@uam.es

The biocompatible properties of titanium nitride (TiN) have opened a new field of applications for this material. In the present work, TiN coatings with thicknesses around 1 μm have been prepared by DC magnetron sputtering. The aim has been to evaluate the adherence, growth and proliferation of human pluripotent mesenchymal stem cells (hMSCs) on the surface of TiN films with contrasted structural, electrical, and mechanical properties. For this purpose, the films were characterized by X-ray diffraction, scanning electron microscopy, sheet resistance measurements, and nanoindentation. Biological tests show that hMSCs adhere and proliferate onto TiN surfaces. The combination of the mechanical, electrical, and biological responses suggest that TiN coatings present appropriate properties to induce the *in vitro* stimulated differentiation of hMSCs. This possibility gives an added value to TiN based biomaterial coatings.

1. Introduction

The physicochemical properties of titanium nitride (TiN) thin films have recently led to the study of the biocompatibility of this material. In effect, TiN coatings present a high corrosion resistance [1] and if deposited on high-speed-steels significantly improve their wear resistance [2]. These two factors are of extreme importance in the field of load bearing prostheses as they determine in the long run the formation of debris, and thus the lifetime of the prostheses. TiAlV alloys, mainly used in prosthetics because of their compatible Young's modulus and high corrosion resistance, have been previously coated with TiN. Ion implantation [3, 4], PACVD [5] and reactive r.f. sputtering [6] deposition techniques have been often used to produce TiN coatings for biomedical applications. Former studies showed that the wear resistance of the TiAlV alloys was considerably increased by the TiN coatings [3, 5], and the corrosion tests carried out by potentiodynamic polarization in simulated body fluids showed also an enhanced resistance to chemical attack [4]. The latter study, comparing the hemocompatibility of different hard coatings, tested the performance of diamond like carbon coatings with respect to TiN [6]. Other tests performed with TiN coated biomaterials compared the *in vivo* and *ex vivo* interaction of TiN surfaces with leukocytes and the adsorption of proteins [7] and concluded that TiN surfaces could be considered as a suitable blood contacting material. The combination of these properties suggest that the TiN coatings can play a barrier function on TiAlV alloys avoiding the negative effects of the Al and V ions, which are produced in the biological media by wear or diffusion processes [8]. As it is evident, a knowledge of the mechanical properties of TiN coatings should be crucial for their application in biological media. Concerning the *in vivo* applications derived from its good electrical conductivity, TiN electrodes with fractal surfaces have been tested for cardiostimulation allowing to monitor the neural response of the myocardium [9]. All these works suggest that the electrical properties, combined with the biological response of cells, make this material very suitable for developing substrates for the stimulated differentiation of human mesenchymal stem cells (hMSCs). Pluripotential hMSCs, which are present in the bone marrow, contribute to the regeneration processes of mesenchymal tissues including cartilage, bone, muscle, ligament, tendon, and stroma [10, 11].

*Author to whom all correspondence should be addressed.

However, several limitations have been pointed out by tissue engineers when the material has to support the differentiation process of the cells [12]. Electromagnetic signaling methods have been reported among the processes used to induce mesenchymal cell differentiation [13]. The exploration of the interaction between TiN coatings and hMSCs must be thus considered of primary interest in the field of tissue engineering.

The aim of this work is to describe the adhesion and proliferation of pluripotential hMSCs onto DC sputtered TiN films with contrasted structural, electrical, and mechanical properties. For the former, hMSCs have been seeded and observed *in situ* on the TiN surface. In order to fully characterize the TiN coatings, we have used X-ray diffraction (XRD), scanning electron microscopy (SEM), sheet resistance measurements and nanoindentation techniques. In particular, the last technique, which has been successfully applied to characterize human cortical and trabecular lamellar bone [14], allows not only the determination of the hardness (H) and Young's modulus (E_m), but also the plastic energy of deformation (PED). In fact, this quantity can be related with the dominant mechanism involved during the indentation process [15].

2. Experimental procedure

2.1. Preparation, structural, and electrical characterization of the TiN coatings

High purity titanium targets (Kurt J. Lesker, 99.99%) were used as sputtering source in an Ion-Tech system. Several sessions of 30 min simultaneous DC sputtering depositions $(Ar/N_2 = 9/1)$ on four Si (1 0 0) substrates with a power of 300 W and chamber pressure of 1.5×10^{-3} mbar led to TiN coatings of approximately 1 μm thickness. Some of these coatings where then sintered by rapid thermal annealing in a N_2 atmosphere at 300, 400, and 600 °C (background pressure 5×10^{-2} mbar). The structural characterization of the coatings was carried out by XRD in a θ/2θ Siemens diffractometer with the following characteristics: 0.04°/step, 6 s/step. SEM micrographs were performed in a Philips XL30 operated at 15 kV, which allowed the measurement of the coatings thickness from cross-sectional views. The sheet resistance measurements were performed by the four-probe method in the $-1, 1$ mA current range.

2.2. Mechanical characterization

Indentation tests were performed in a Shimadzu DUH-200 dynamic ultra microhardness tester with resolutions of 0.02 mN in load and 0.01 μm in depth. Initially, six loading–unloading tests up to 20 mN were applied to every sample to obtain PED values (area of the load–unload hystheresis loop) of the as prepared and sintered TiN coatings. Secondly, for the calculation of H and E_m, maximal loads of 6, 10, 15, and 20 mN were applied. The samples were probed six times with a Berkowich diamond tip indentor. These indentations consisted of five loading cycles allowing a 40% unload after 1 s. H and E_m were determined following the method described by Oliver and Pharr [16]. The basis consists in the introduction of geometrical and experimental corrections to the analytic expression used for the calculation of the projected area of contact, which is obtained from the estimation of the depth of contact. The tip area had been previously calibrated using quartz and aluminum references.

2.3. Adhesion of hMSCs

In order to evaluate the adhesion and proliferation of hMSCs on TiN in comparison with bare TiAlV surfaces, pluripotential hMSCs were isolated from adult bone marrow following a standard procedure [17]. hMSCs were seeded in DMEM-low glucose supplemented with 10% fetal bovine serum (FBS). After culture, hMSCs were found to form colonies. Finally, after three weeks, the cells were harvested by treatment with 0.05% trypsin/0.53 mM EDTA during 5 min and collected by centrifugation.

The TiN and TiAlV surfaces were washed with phosphate buffer saline (PBS) and sterilized by overnight exposure to UV in a tissue culture cabin. About 2×10^5 hMSCs were seeded on 6 mm diameter disks of TiN coating and TiAlV surfaces and incubated during 48 h at 37 °C in O_2/CO_2 (96/4, V/V) atmosphere. Finally, the samples were washed with PBS and the cells were fixed with methanol.

In order to visualize the samples, a fluorescence reaction was induced using an autoimmune serum from bGH transgenic mice and an anti-mouse IgG secondary antibody labeled with fluorescein [18]. Briefly, the surfaces were blocked with 5% milk protein in TBST (10 mM Tris–HCl pH 7.5, 150 mM NaCl and 0.05 Tween 20) during 2 h. Then, 200 μl of autoimmune serum (1/200 dilution) were placed on each surface during 5 h and after this incubation period the surfaces were washed with 1% milk protein in TBST. The reaction with the secondary antibody (1/4000 dilution) was carried out during 30 min in dark conditions. After washing the secondary antibody, the cells were visualized under 495 nm illumination in a fluorescence microscope Axiovert 35.

3. Results

3.1. Structure and composition

The XRD diagrams corresponding to as-deposited TiN (TiN-AS) and annealed films (TiN-300, TiN-400, TiN-600) showed, as monitored in Fig. 1, the presence of a weak (1 1 1) TiN cubic phase with almost non-detectable (2 0 0) peaks. This effect is a consequence of the preferential growth of the coatings in the (1 1 1) direction as deduced from the comparison with reported intensity charts (PDF 38-1420). The annealing treatments at 300 and 400 °C produced only a slight increase of the (0 0 2) peak but did not produce a critical enhancement of the film crystallinity. Sintering at 600 °C activated a densification process as derived from the slight change of intensity of the (1 0 0) peak at $2\theta = 36.65$.

The SEM micrographs from the TiN films show extremely homogeneous coatings as depicted in Fig. 2. The top view image (Fig. 2(a)), which was focused with the reference of an induced surface mark, shows the absence of relevant surface roughness at the μm scale.

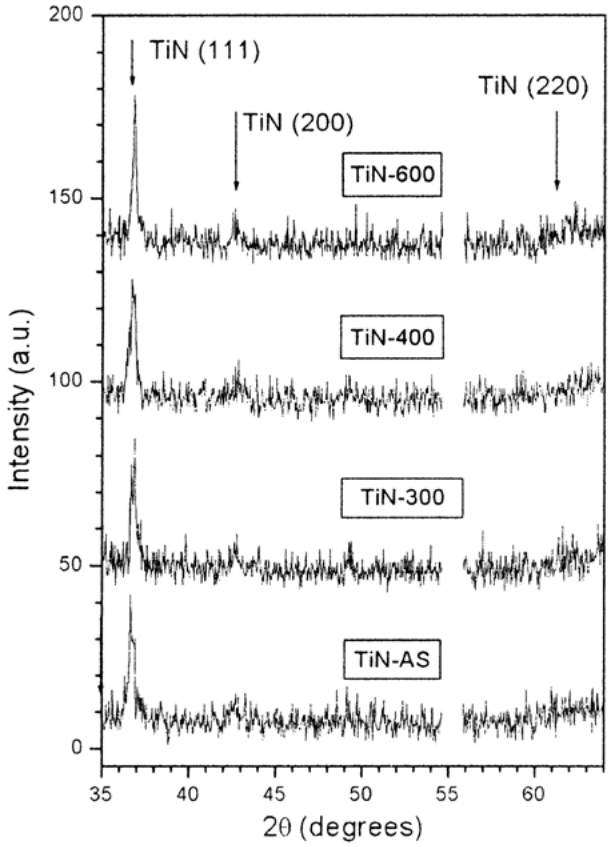

Figure 1 XRD diagrams from TiN-AS, TiN-300, TiN-400 and TiN-600 coatings.

This fact was also confirmed for the coatings sintered at higher temperatures. The cross-section image shown in the inset (Fig. 2(b)) was obtained from backscattered electrons, which are sensible to the species present in a compound although the images present lower spatial resolution. This image confirmed that the final thickness of the coating is of the order of 1 μm, in agreement with the estimations obtained from the sputtering growth rate.

The I–V sheet resistance characteristic curves from the TiN coatings presented a linear behavior in the $-1,1$ mA range. The TiN-AS, TiN-300 and TiN-400 presented similar sheet resistance values of about 60 Ω/□. Only the TiN coatings sintered at 600 °C presented slightly lower sheet resistance values of 45 Ω/□.

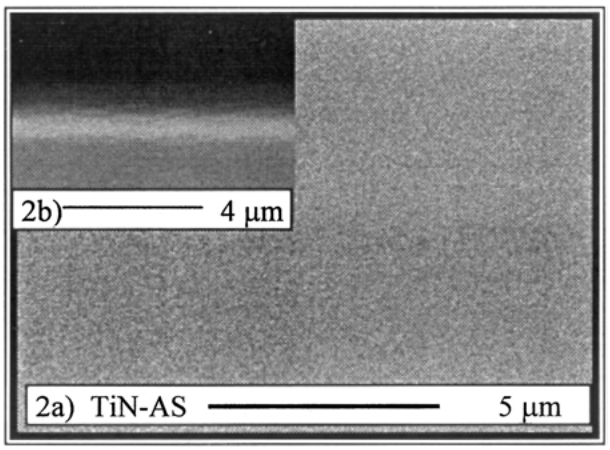

Figure 2 SEM images from the TiN-AS sample. (a) Top view. (b) Cross-sectional view in the backscattered electron mode.

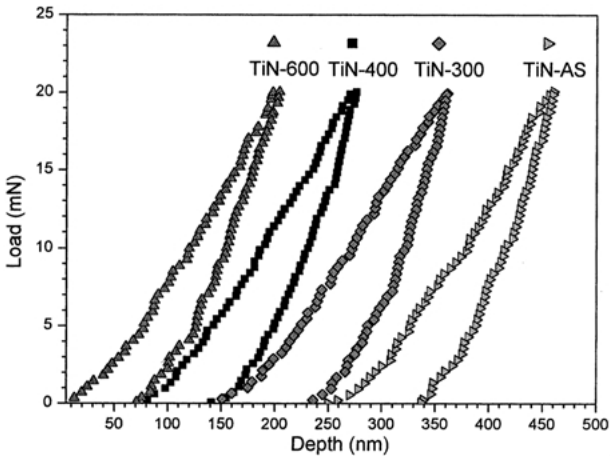

Figure 3 Full loading–unloading versus depth curves in tests with maximal loads of 20 mN. TiN-AS, TiN-300, TiN-400, TiN-600.

3.2. Mechanical properties

Typical 20 mN loading – unloading versus displacement curves for different coatings are presented in Fig. 3. It is observed that all the coatings present very similar mechanical behavior. The PED values are presented in the first column of Table I and can serve to establish the slight mechanical differences existing between the samples. The error of the PED values was determined from the standard deviations after six measurements on each sample rather than derived from the apparatus precision. These values show that annealed coatings exhibit a slightly lower plastic deformation (760 pJ) than the TiN-AS coatings (1000 pJ). The mechanical similarities are also evidenced from the closeness of the values of maximal indentation depth and unloading slope. The annealed TiN-600 coatings are somewhat stiffer since they present smaller maximal depths and higher unloading slopes than the other coatings, as discerned from the loading – unloading charts of Fig. 3. The mechanical similarity between the coatings is confirmed by the calculation of the values of H and E_m, which are listed in Table I. The values of H were observed to be only slightly dependent on indentation depth reaching a maximum value for maximal loads of 20 mN (second column, Table I). The E_m values are independent of the indentation load as derived from the model of Oliver and Pharr [16]. It can be also observed that both H and E_m increase slightly for increasing annealing temperature (from 18.8 to 19.5 GPa and from 286 to 310 GPa for H and E_m, respectively).

3.3. Adhesion of hMSCs

In order to establish a comparative test, we analyze the adherence and growth of cells on TiN surfaces in

TABLE I Values of the most important mechanical parameters obtained from different coatings

Sample	PED (pJ)	H (GPa)	E_m (GPa)
TiN-AS	1000 ± 40	18.8 ± 0.7	286 ± 8
TiN-300	920 ± 40	18.9 ± 0.8	299 ± 8
TiN-400	890 ± 40	19.2 ± 0.9	300 ± 20
TiN-600	760 ± 40	19.5 ± 0.9	310 ± 20

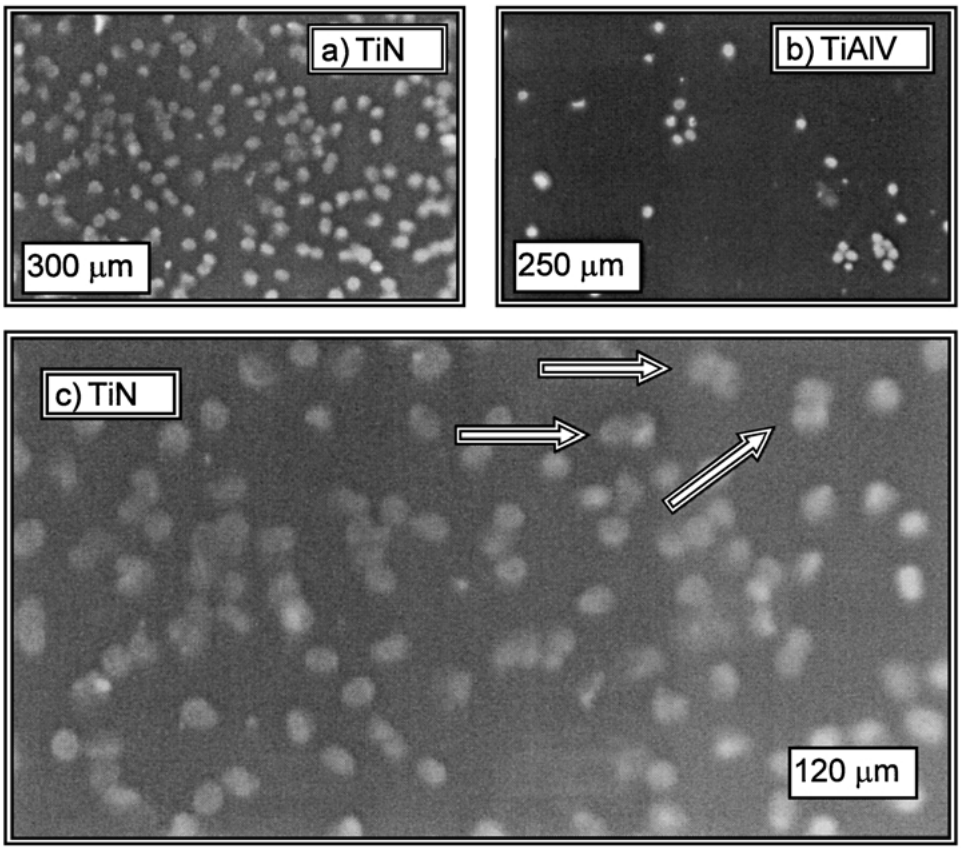

Figure 4 Fluorescence micrograph showing hMSCs seeded on (a) TiN-AS, (b) TiAlV alloy, (c) magnification of TiN-AS.

comparison with TiAlV surfaces. In view of the stability of the TiN coatings to the annealing treatments, the tests are primarily focused in the study of TiN-AS coatings. The hMSCs on TiN and TiAlV surfaces do react with the autoimmune serum since the images in Fig. 4 show that the antinuclear and anti-cytoskeleton antibodies recognize the human homologous proteins (i.e. the fluorescent reaction is concentrated in the cell nuclei). As it can be observed, cells adhere both TiN and TiAlV surfaces (Fig. 4(a) and (b)). It was established that almost 90% of the cultured cells adhere onto TiN. However, the corresponding value for hMSCs on TiAlV surfaces is about 40%. The nuclei present no apoptotic signs and their geometry was consistent with that of normal hMSCs in culture. The nuclei of the hMSCs form isolated groups on TiAlV surfaces (Fig. 4(b)) which have been identified with a previous stadium of growth of the cells. The cells on the TiN surface have overcome that stadium and present a tendency to be homogeneously distributed over the surface. Nevertheless, several nuclei can be observed at higher magnifications forming pairs (arrows, Fig. 4(c)), a fact which is interpreted as a proof of the hMSCs activity while adhered on TiN. These results support the notion of improved surface properties of DC sputtered TiN in comparison with the TiAlV surface for the development of hMSCs.

4. Discussion and conclusions

The TiN coatings formed in this work by DC sputtering have been found to present very stable structures and morphologies, even after annealing at 300, 400, and 600 °C, as derived from XRD and SEM results. For all the TiN coatings, the low substrate temperature involved during processing induced a preferential growth of the coating along the (1 1 1) direction [19]. Only a slight densification process, accompanied by a diminution of the sheet resistance could be observed on the TiN600 sample as a relevant structural feature. This densification process has been previously observed with a transition temperature around 450 °C on sputtered TiN thin films [20]. The values of sheet resistance are in all the cases higher than those obtained for similar coating thickness in applications concerning very large scale integration in microelectronics [21]. The reduction of the sheet resistance after sintering at 600 °C can be understood in terms of the formation of an interfacial titanium silicide film [22], although there is no experimental evidence of this effect on our TiN coatings. Indentation tests have shown that the structural similarity existing between the as-prepared and annealed TiN coatings correlate with a very similar mechanical behavior. The values of H and E_m remain similar within the experimental error although it has been established that coatings sintered at 600 °C suffer from lower plastic deformations. In other words, TiN coatings sintered at 600 °C present a more pronounced elastic indentation mechanism [15].

The comparison of the mechanical properties of these coatings with those from other TiN films produced by alternative methods reveals the high performance of our coatings. The values of H and E_m measured by nanoindentation on TiN thin films prepared by the dynamic ion mixing technique [23] gave very low values of both H and E_m ($H = 4$ GPa and $E_m = 200$ GPa) in comparison with the results obtained in the present work. The results for planar magnetron sputtered coatings with

different crystalline orientations are closer to the values obtained in our study [24]. The values of H of such obtained coatings (20 GPa) are quite close to the values of our TiN coatings although a relevant dispersion was found for values of E_m (450 GPa). In general, it has been concluded from flexural resonant frequency studies that the maximal values of E_m for TiN_x coatings is obtained for $x = 1$ and reaches values of up to 640 GPa [25]. Although this may indicate some deficiency in N content in our coatings, we consider that the huge dispersion obtained in the cited values could be partially explained by the differences between the measurement systems.

The results from hMSCs seeding prove that reactively sputtered TiN coatings present improved surface properties with respect to the traditional TiAlV alloys, since a considerably higher number of hMSCs was observed to adhere onto the TiN surface. The combination of the electrical, mechanical, and biological results of TiN coatings is considered of primary interest for prosthetic applications. DC sputtered TiN coatings deposited on TiAlV alloys can not only act as functional diffusion barriers avoiding the negative effects of Al and V ions, but they can also play an active biological role. Moreover, high levels of adhered hMSCs can be obtained *in vitro* and the differentiation of these cells (i.e. into functional osteoblasts) can be stimulated *in situ* by electric pulses or upon implantation. The electrical properties of the TiN coatings suggest that this stimulation of the cellular differentiation can be achieved prior to implantation. A cellular pretreatment of the prostheses surface can thus considerably enhance the bone–TiN interface at the early stages of implantation.

Acknowledgments

M. Manso thanks the Regional Government of Madrid for his research grant.

References

1. R. HÜBLER, A. SCHRÖER, W. ENSTNGER, G. WOLF, F. C. STEDILE, W. H. SHREINER and I. J. R. BAUMVOL, *J. Vac. Sci. Technol.* **11** (1993) 451.
2. M. Y. AL-JAROUDI, H. T. G. HENTZELL, S. GONG and A. BENGSTON, *Thin Solid Films* **195** (1991) 63.
3. F. TORREGROSA, L. BARRALLIER and L. ROUX, *ibid.* **2** (1995) 245.
4. H. SCHMIDT, C. KONETSCHNY and U. FINK, *Mater. Sci. Tech.* **14** (1998) 592.
5. K. T. RIE, T. STUCKY, R. A. SILVA, E. LEITAO, K. BORDJI, J. Y. JOUZEAU and D. MAINARD, *Surf. Coat. Technol.* **32** (1995) 973.
6. M. I. JONES, I. R. MCCOLL, D. M. GRANT, K. G. PARKER and T. L. PARKER, *Diamond and Related Mater.* **8** (1999) 457.
7. I. DION, X. ROQUES, N. MORE, L. LABROUSSE, J. CAIX, F. LEFEBRE, F. ROUAIS, J. GAUTREAU and C. H. BAQUEY, *Biomaterials* **14** (1993) 712.
8. M. LONG and H. J. RACK, *ibid.* **19** (1992) 1621.
9. M. SCHLALDACH, *Med. Prog. Technol.* **21** (1995) 1.
10. A. I. CAPLAN, *J. Orthp. Res.* **9** (1991) 641.
11. S. P. BRUDER, A. A. KURTH, M. SHEA, W. C. HAYES, N. JAISWAL and S. KADIYALA, *ibid.* **16** (1998) 155.
12. K. ANSELME, *Biomaterials* **21** (2000) 667.
13. Y. HARAKI, N. ENDO, M. TAKIGAWA, A. ASADA, H. TAKAHASHI and F. SUZUKI, *Biochim. Biophys. Acta* **931** (1987) 94.
14. J. Y. RHO, T. Y. TSUI and G. M. PHARR, *Biomaterials* **18** (1997) 1325.
15. L. E. SAMUELS in ''Microindentation Techniques in Materials Science and Engineering'' (American Society for Testing Materials, Philadelphia, 1986) p. 5.
16. W. C. OLIVER and G. M. PHARR, *J. Mater. Res.* **7** (1992) 1564.
17. D. P. LENNON, S. E. HAYNESWORTH, S. P. BRUDER, N. J. JAISWAL and A. I. CAPLAN. *In Vitro Cell Dev. Biol.* **32** (1996) 602.
18. S. OGUETA, I. OLAIZABAL, I. SANTOS, E. DELGADO-BAEZA and J. P. GARCÍA RUIZ, *J. Endocr.* **165** (2000) 321.
19. J. S. CHUN, I. PETROV and J. E. GREEN, *J. Appl. Phys.* **86** (1999) 3633.
20. K. C. PARK and K. B. KIM, *J. Electrochem. Soc.* **142** (1995) 3109.
21. S. Q. WANG, I. RAAIJMAKERS, B. J. BURROW, S. SUTHAR, S. REDKAR and K. B. KIM, *J. Appl. Phys.* **68** (1990) 5176.
22. A. AMIGLIATO, M. FINETTI, A. GARULLI, S. GUERRI, R. LOTTI and P. OSTOJA, *Thin Solid Films* **129** (1985) 55.
23. T. HAYASHI, A. MATSUMURO, M. MURAMATSU, Y. TAKAHASHI and K. YAMAGUCHI, *ibid.* **349** (1999) 199.
24. H. LJUNGCRANTZ, M. ODÉN, L. HULTMAN, J. E. GREEN and J. E. SUNDGREN. *J. Appl. Phys.* **80** (1996) 6725.
25. E. TÖRÖK, J. PERRY, L. CHOLLET and W. D. SPROUL, *Thin Solid Films* **153** (1987) 37.

Received 24 April
and accepted 7 September 2001